Beam Size Measurement in Linear Colliders using a Gradient Undulator and Off-Axis Detection.

E. G. Bessonov*, N. J. Walker and S. G. Wipf
Deutches Elektronen Synchrotron DESY
Notkestr. 85, 22603 Hamburg Germany.

* Lebedev Physical Institute AS, Moscow, Russia.

Abstract

The underlying theory of the Gradient Undulator beam size monitor as proposed in [1] is given. It is shown that there is an easily detectable signal at relatively large angles (compared to $1/\gamma$ of the electron beam) which should enable the device to be operated in a straight linac using an annular detector positioned several meters downstream. Operational aspects of the device, as well as tolerance issues and sources of background are also discussed.

1 Introduction

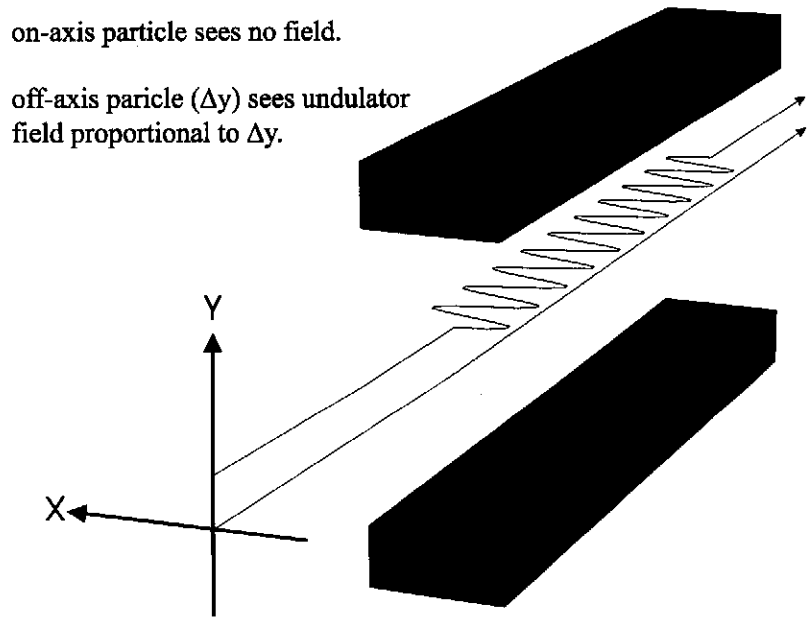

Figure 1: Concept of the Gradient Undulator Beam Size (GUBS) monitor as described in [1].

Beam size measurement in next generation electron-positron linear colliders is a key issue to preserving the extremely small emittances required by these ambitious accelerators. In [1] a novel technique using a *Gradient Undulator* was described,

which enables the *rms* of a single bunch of the electron (positron) beam to be measured.

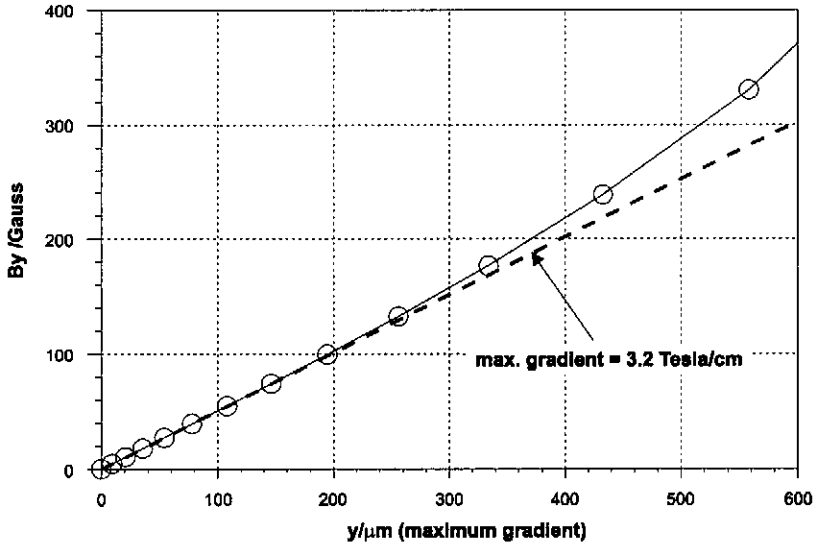

Figure 2: MAFIA field calculation as a function of vertical offset at the maximum field gradient (for undulator parameters see table 1).

Beam sizes of the order of 5-20 μm can easily be resolved to an accuracy of a few percent. The measurement is extremely simple, requiring only the total number of photons to be counted, and is non-invasive. Typical profile measurement techniques using travelling wires or *laser*-wires must sample many pulses in the bunch train to provide a convoluted distribution of the beam: they are not single shot measurements. The gradient undulator on the other hand is a single pulse device, but since it measures the *rms* of the beam, it may be sensitive to long transverse tails. Figure 1 shows the basic concept of the device, while table 1 gives the parameters of the device which were used in [1], with the exception of the field gradient which has since been calculated using MAFIA [2] (figure 2). Unless otherwise stated, these data will form the basic reference set for the following calculations.

length	1.0	Meter
λ_U	1.0	cm
no. of periods	100	
gap	3.0	mm
max. gradient*	3.2	Tesla/cm
typical *rms* beam size**	8.0	μm

Table 1: Properties of the Gradient Undulator described in [1].
*** assumed here is a Samarium-Colbalt hybrid undulator (see fig. 2)**
**** based on the TESLA vertical beam size at the exit of the linac (250 GeV)**

In [1] a chicane based arrangement for the undulator was described. The chicane allowed all the radiated photons to be captured, and had the additional benefit of displacing the detector from the axis of the linac, thus reducing background from the

linac itself. In this paper, we give a more in depth derivation of the theory, and show that it is possible to use the device in a straight linac with a ring detector as depicted in figure 3 (so-called off-axis mode). We will show that even though the angle subtended by such a detector is many times larger than the characteristic angle associated with radiation from an undulator (~1/γ), there is still an easily detectable number of photons at these angles. Finally tolerance, background and operational issues will be discussed.

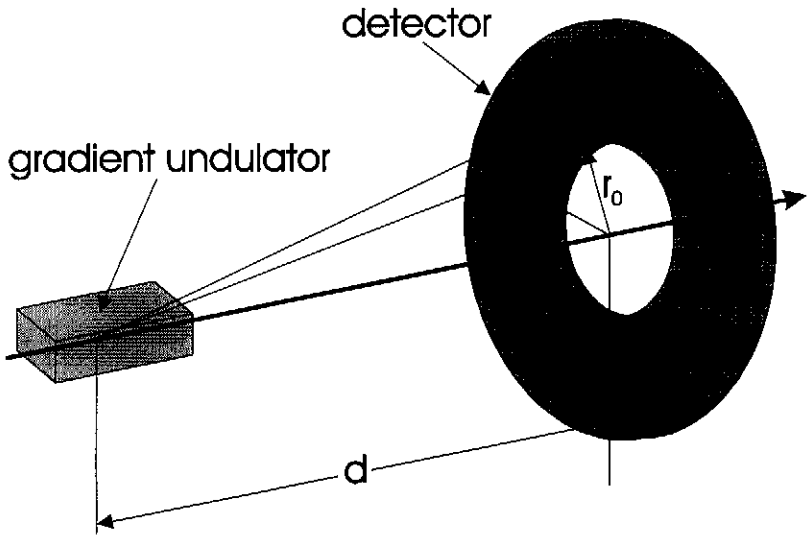

Figure 3: Schematic of off-axis detection scheme (not to scale).

2 Review of basic undulator theory

We provide here a review of the underlying theory that is pertinent to estimating the total number of photons expected from the device under nominal operating conditions. For a more complete theory, see (for example) [3,4].

2.1 A Note on Units

Publications dealing with the theory of undulator radiation generally use the *cgs* or *Gauss* system of units. In the following sections, the *MKS* system of units is used, unless otherwise stated.

2.2 Total Radiated Energy

The total energy radiated by an electron (positron) traversing a given magnetic field B of finite length L is given by

$$E_R = \frac{e^2 c^2}{2\pi} C_\gamma \gamma^2 \langle B^2 \rangle L, \qquad (1)$$

where $\langle B^2 \rangle$ is the variance of the magnetic field along the length of the undulator (L), γ is the relativistic factor E/mc^2 and the constant C_γ is given by

$$C_\gamma = \frac{4\pi}{3}\frac{r_e}{mc^2} \approx 2.31\times10^{-11}\ \mathrm{m/GeV}. \qquad (2)$$

All other symbols have their standard meanings. For a harmonic undulator, we can replace $\langle B^2 \rangle$ by $B_0^2/2$, where B_0 is the peak of the undulator field. In the case of the gradient undulator B_0 is given by $G\cdot\Delta y$, where Δy is the vertical offset of the radiating particle, and G is the maximum field gradient dB_0/dy: hence

$$E_R = \frac{e^2c^2}{4\pi} C_\gamma \gamma^2 G^2 \Delta y^2 L. \qquad (3)$$

For the parameters given in table 1, with $\gamma = 5\times10^5$ and $\Delta y = 8$ μm (corresponding to the beam height at the exit of the TESLA linac), we have $E_R = 4.34\times10^{-17}$ J[1].

2.3 Angular distribution of radiation

The expression for the wavelength of the undulator radiation is

$$\lambda_k = \frac{\lambda_u}{2k\gamma^2}(1 + p_{\perp m}^2 + \gamma^2\theta^2), \qquad (4)$$

where λ_k is the wavelength of the k^{th} harmonic, λ_u is the period of the undulator, θ the azimuthal angle and $p_{\perp m}$ is the *deflection parameter* given by

$$p_{\perp m} = \frac{eB\lambda_u}{2\pi mc} \approx \frac{B[Tesla]\lambda_u[cm]}{1.07}. \qquad (5)$$

Since the fields under consideration here are on the order of $\sigma\times G \approx 25$ Gauss, we are clearly in the regime where $p_{\perp m} << 1$. As a consequence, almost all radiation is emitted at the fundamental (k=1), and to a good approximation we can write (4) as

$$\lambda = \frac{\lambda_u}{2\gamma^2}(1 + \gamma^2\theta^2). \qquad (6)$$

[1] For TESLA this corresponds to an average power of ~9 mWatt.

The bandwidth of the radiation ($\Delta\lambda/\lambda$) is given by $(kK)^{-1}$, where K is the total number of undulator periods. Thus if K>>1, we can assume that all the power is radiated at the fundamental, and at a wavelength which is uniquely given by the azimuthal angle θ in accordance with (6) (see figure 4).

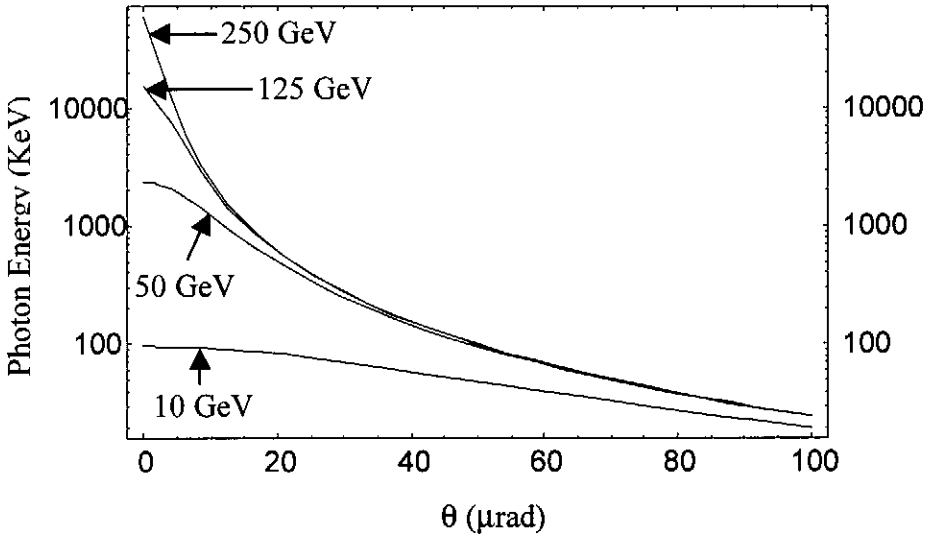

Figure 4: Photon energy as a function of azimuthal angle for various electron energies.

2.4 Undulator spectrum

In the regime of small $p_{\perp m}$, the spectrum of the radiation emitted by a plane undulator with a harmonic magnetic field is given by

$$\frac{dE}{d\xi} = E_R f(\xi), \tag{7}$$

where $\xi = \lambda_{min}/\lambda = \omega/\omega_{max}$, $(0<\xi\leq 1)$, $\int f(\xi) d\xi = 1$, and

$$f(\xi) = 3\xi(1-2\xi+2\xi^2). \tag{8}$$

From (6), we have $\lambda_{min} = \lambda_u/2\gamma^2$, and

$$\xi = \frac{1}{1+\gamma^2\theta^2}. \tag{9}$$

The energy radiated into the frequency interval (ξ_1, ξ_2) is thus given by

$$\Delta E = \int_{\xi_1}^{\xi_2} \frac{dE_R}{d\xi} d\xi$$
$$= \int_{\xi_1}^{\xi_2} E_R f(\xi) d\xi . \qquad (10)$$

Combining equations 9 and 10, with a suitable change of variable from ξ to θ, we have

$$\Delta E = \int_{\theta_2}^{\theta_1} E_R g(\theta) d\theta , \qquad (11)$$

where ($\theta_1 < \theta_2$), and

$$g(\theta) = \frac{6\gamma^2\theta(1+\gamma^4\theta^4)}{(1+\gamma^2\theta^2)^5} . \qquad (12)$$

2.5 Total number of photons emitted

The total number of photons emitted into angular interval (θ_1, θ_2) is given by

$$\Delta n_\gamma = \int_{\theta_2}^{\theta_1} \frac{E_R}{\hbar\omega} g(\theta) d\theta = \int_{\theta_2}^{\theta_1} \frac{\lambda E_R}{2\pi c\hbar} g(\theta) d\theta . \qquad (13)$$

Substituting (6) for λ, (3) for E_R, and (12) for $g(\theta)$, the integrand in (13) becomes

$$\frac{3ce^2 C_\gamma B_0^2 L\lambda_u}{4\pi h}\left[\frac{\gamma^2\theta(1+\gamma^4\theta^4)}{(1+\gamma^2\theta^2)^4}\right]. \qquad (14)$$

Integrating (14) from $\theta = 0$ to $\theta = \infty$ gives the total number of photons emitted (n_γ):

$$n_\gamma = \frac{ce^2 L B_0^2 C_\gamma \lambda_u}{4\pi h} \approx 1.33 \times L[\mathrm{m}] B_0^2[\mathrm{Tesla}^2]\lambda_u[\mathrm{cm}] \qquad (15)$$

It is interesting to note that this result is independent of energy, and depends only on the physical characteristics of the undulator. Again for the gradient undulator we can replace the peak field B_0 by $G \cdot \Delta y$.In practical units, the total number of photons per 10^{10} electrons can then be expressed as

$$n_\gamma = 133.\times G^2[\text{Tesla}^2/\text{cm}^2]\Delta y^2[\mu\,\text{m}^2]L[\text{m}]\lambda_u[\text{cm}]. \qquad (16)$$

Again for our standard parameter set, n_γ is approximately 9×10^4 photons per 10^{10} electrons.

2.6 Number of photons in a finite angle

For the off-axis detection scheme, we consider an annular detector centered on the beam axis that subtends a finite azimuthal angle from θ_{min} to θ_{max}. Integrating (14) gives

$$\Delta n_\gamma = \left[\frac{ce^2C_\gamma LB_0^2\lambda_u}{8\pi h}\left[\frac{2+3\gamma^2\theta^2+3\gamma^4\theta^4}{(1+\gamma^2\theta^2)^2}\right]\right]_{\theta_{min}}^{\theta_{max}}. \qquad (17)$$

In the limit $\gamma\theta>>1$ the implicit integral (17) falls of as $1/\theta^2$: thus assuming that $\theta_{max}>>\theta_{min}$, we can approximate (17) as

$$\Delta n_\gamma \approx \left[\frac{3ce^2C_\gamma LB_0^2\lambda_u}{8\pi h\gamma^2\theta^2}\right]_{\theta_{min}}^{\theta_{max}} \approx \frac{3ce^2C_\gamma LB_0^2\lambda_u}{8\pi h\gamma^2\theta_{min}^2}. \qquad (18)$$

In terms of the field gradient (G) and particle offset (Δy), the number of photons per 10^{10} electrons is given (in practical units) as

$$\Delta n_{\gamma,\infty} \approx (2.0\times10^{14})\times\frac{L[\text{m}]G^2[\text{Tesla}/\text{cm}^2]\Delta y^2[\mu\,\text{m}^2]\lambda_u[\text{cm}]}{\gamma^2\theta_{min}^2[\mu\,\text{rad}^2]}. \qquad (19)$$

For a minimum angle $\theta_{min} = 10\,\mu\text{rad}$, we have $\Delta n_{\gamma,\infty} \approx 5\times10^3$ photons per 10^{10} electrons[2] ($\gamma = 5\times10^5$), still an easily detectable signal even though it is a factor of 17 smaller than the total number of quanta emitted. We should also note that the characteristic angle $1/\gamma$ is approximately 2μm, a factor of five smaller than θ_{min}. Figure 5 shows the number of photons as a function of θ_{min} for various electron energies.

[2] Note that in this case, $\gamma^2\theta^2_{min} = 25$, and so our approximation in deriving (18) is justified.

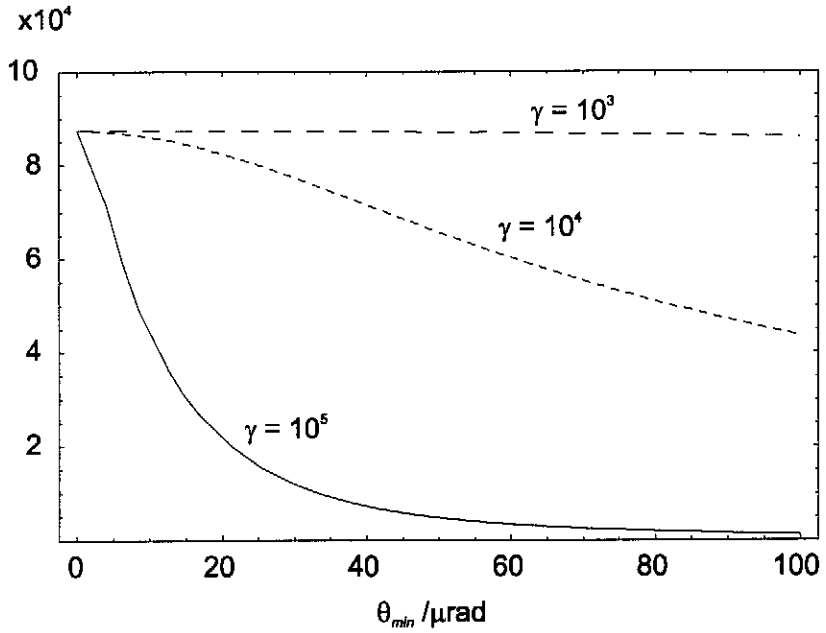

Figure 5: Total number of photons generated as a function of the minimum azimuthal angle for various electron energies.

3 Mode of Operation

Although the mode of detection is slightly different between the chicane based proposal outlined in [1] and the off-axis detection suggested here, the actual mode of operation of the device itself is the same in both cases. The gradient undulator will be placed on a vertical precision mechanical mover, allowing the vertical offset of the beam with respect to the undulator to be scanned. In addition, a precision BPM is attached to the undulator, which is used to correct pulse to pulse current and position jitter during a measurement. The number of photons radiated is given by

$$n_\gamma = aN\left(\sigma_y^2 + \Delta_y^2\right), \tag{20}$$

where Δ_y is the vertical displacement of the mover, a is a constant of proportionality (which can be determined experimentally from a parabolic fit of the scan data), and N is the number of particles (current). The constant a depends on the following physical characteristics:

- the undulator parameters (L, λ_u, dB_0/dy)
- the beam energy (γ)
- the geometry of the detector (r_0, r_1 and d in figure 3).

The latter two points are only applicable to the off-axis detection scheme shown in figure 3. If we assume a to be constant over time, it is then possible to make *single-shot* measurements of single bunches. The first stage is to make a calibration of the undulator by vertically scanning the position, and measuring the resulting signal. Fitting (20) to the resulting data enables us to

1. determine the constant a
2. determine the axis of the undulator, and calibrate the attached BPM accordingly.

Once complete, the vertical position of the undulator is adjusted to centre the beam on the undulator axis. Beam jitter (both current and position) can be measured by the BPM on a shot-to-shot basis, and used to correct the measured beam size.

4 Tolerances

The issue of mechanical and field tolerances for undulators has been dealt with in some depth in [3] and [6]. In both these publications the authors are primarily concerned with the effect on the spectrum and quality of the radiation. In the present application, we are only interested in the total power generated by the device, and not in the spectral quality of the light produced.

4.1 Global alignment tolerances

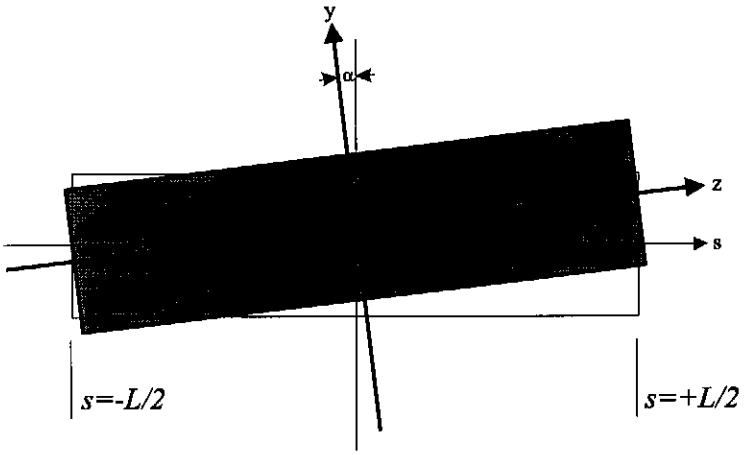

Figure 6: Geometry of alignment errors, showing a net vertical displacement Δ and a pitch error α.

There are several tolerances that are of issue here. Alignment of the device with respect to the beam can be achieved using scanning techniques of the mechanical mover. The tolerance on the net vertical alignment is effectively given by the beam size in accordance with (20). Since the effect on the measurement of an alignment error adds in quadrature with the beam size, we have a relative (systematic) error in the measurement given by

$$\frac{\delta\sigma_y}{\sigma_y} \approx \frac{1}{2}\left(\frac{\Delta}{\sigma_y}\right)^2. \qquad (21)$$

Hence with $\sigma_y = 8$ μm, an offset of 2 μm gives a systematic error of ~3%. The correct beam alignment can be determined from the mover scan, after which an orbit feedback can keep the beam centred on the device.

The effect of the pitch angle (α) can be estimated by integrating over the offset of the device, which is now a function of the longitudinal position s (see figure 6):

$$n_\gamma = \frac{aN}{L}\int_{-L/2}^{L/2}\left[\sigma_y^2 + (\Delta + \alpha s)^2\right]ds$$
$$= aN\left(\sigma_y^2 + \Delta^2 + \frac{\alpha^2 L^2}{12}\right) \quad . \tag{22}$$

If the mechanical mover also allows the adjustment of the pitch of the device (*e.g.* two separate vertical movers at either end of the undulator), the angle α can also be scanned and the signal minimised. For a 1 meter long device, an angle of ~7 μrad gives the equivalent tolerance of a net offset of 2 μm.

A final "global" alignment tolerance that should be considered is the tilt of the device (*i.e.* the rotation about the z-axis). Bearing in mind that the number of photons generated is proportional to B^2, we can estimate the ratio of photons from the horizontal beam size (σ_x) to the vertical beam size of interest (σ_y) as

$$\frac{n_{\gamma,x}}{n_{\gamma,y}} \approx \left(\frac{\sigma_x}{\sigma_y}\right)^2 \phi^2, \tag{23}$$

where ϕ is the tilt angle. Assuming a tolerance of 1% for the ratio and a typical linac (fodo) ratio[3] for σ_x/σ_y of ~5, we obtain a relatively relaxed tolerance of approximately 20 mrad.

4.2 Mechanical tolerances

So far we have dealt with global alignment tolerances of the device as a whole: in principle these effects can be "tuned" out using high precision mechanical movers and accurate beam position monitors (typical resolutions of which can be a few microns). The effect of random pole alignment and field errors can not in general be tuned out, and will always lead to a systematic error in the measured beam size. Following a similar analysis for the global alignment errors, we can show that *effective random alignment errors*[4] (δ^2_{rms}) lead to an additional term added in quadrature to the measurement:

$$n_\gamma = aN\left(\sigma_y^2 + \Delta^2 + \frac{\alpha^2 L^2}{12} + \delta^2_{rms}\right). \tag{24}$$

[3] We assume here that the undulator is placed close to a defocusing quadrupole, and thus at a β_y maximum point (β_x minimum).

[4] We included here not only physical displacement of the poles, but intrinsic field errors which can be expressed as an effective offset.

As with the net displacement Δ, an effective *rms* pole alignment error of 2 μm will give a systematic error of ~3% in σ_y (= 8 μm).

5 Detectors

The energy of the generated photons depends of the energy of the electron beam, and consequently can vary from a few keV at the low energy end of the machine to ~60 MeV at the exit of the linac. Depending on the energy of the photons, different detectors can be utilised. The most suitable detectors of γ-rays in the energy range 0.1-100 MeV are the scintillator and Cherenkov detectors [7]. In this case, the photons are first passed through a radiator or converter in which they generate secondary electrons or electron-positron pairs. These particles are subsequently passed through a scintillator or Cherenkov radiator where they generate optical photons that can be easily detected using photomultipliers. A possible arrangement for such a scheme is shown in figure 7. For X-ray radiation, silicon photodiodes as well as other semiconductor devices can be used [7].

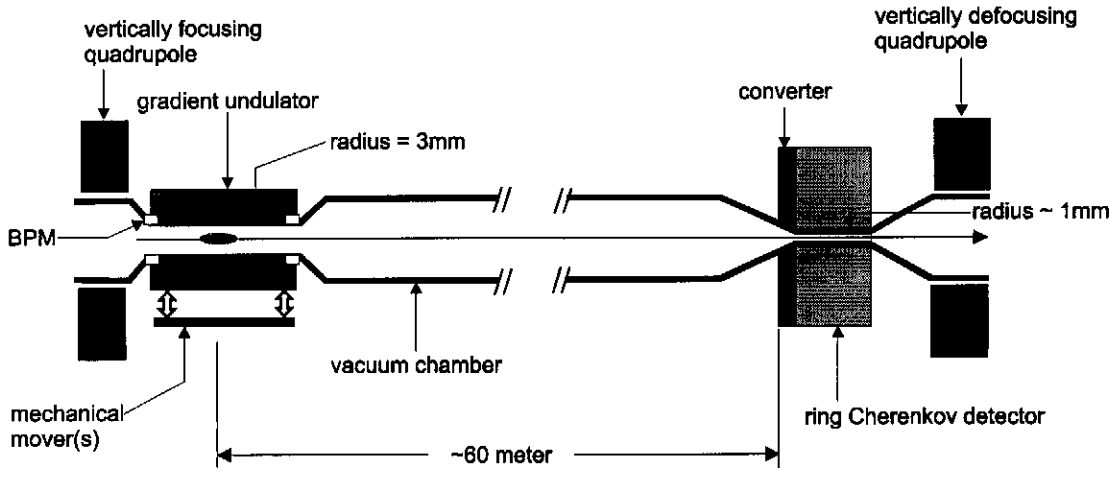

Figure 7: Schematic of a GUBS monitor used in an off-axis detection mode (the half-cell length and detector aperture reflects the typical 250 GeV case).

6 Background

Assuming that we have an arrangement similar to that shown if figure 7, the predominant source of background is likely to be from the "short magnet" radiation from the quadrupoles [8]. The largest contribution comes from the vertically defocusing quad at the position of the undulator (see figure 7). The intensity and spectral properties of this radiation depends on the alignment of the beam with respect to the quadrupole. For a well-aligned quadrupole, this background has been estimated to be negligible, however, further investigation of potential background sources is still required.

7 Conclusion

A one-meter gradient undulator with a period of 1 cm can be used to produce a single bunch measurement of the *rms* beam height of a high-energy electron (positron) beam, as is typically found in a linear collider. Beam sizes of the order of 5-20 μm can be resolved with an accuracy of a few percent, providing that mechanical tolerances on the order of a few microns for the undulator can be achieved. Typical numbers of photons per pulse are in the range of 10^3 to 10^6 per 10^{10} electrons, while characteristic photon energies for electrons energies of 50-250 GeV are in the range 1 to 60 MeV. Below electron energies of ~30 GeV, the photon energy drops to a few 100 KeV. An off-axis detection scheme using a ring detector has been shown to be feasible, even though the subtended azimuthal angle at the undulator (typically 10 μrad) is significantly larger than $1/\gamma$. Background issues for such a detector placed close to the axis of the accelerator (some 100 times the nominal beam size) are still a question: sources of 10-60 MeV photons need to be identified and their impact on the detector quantified. At present, only *short-magnet* radiation due to the quadrupoles in the linac lattice has been investigated, and this background source appears to be negligible. One potential problem of the device is its sensitivity to beam tails, since the undulator signal is proportional to the true variance of the beam distribution. Therefore, this device should be considered complementary to profile monitors (such as mechanical- or laser-wire scanners), which require many beam pulses for a single measurement, but do provide information about the distribution of the core of the beam.

8 References

1. E. G. Bessonov, J. Pflüger, G.-A. Voss, N. J. Walker, *Beam Size Measurements in a Linear Collider using an X-ray Gradient Undulator*, Internal DESY report M96-18, September 1996.
2. The MAFIA Collaboration, *Users' Guide MAFIA Version 4.1*, CST GmbH, Lautenschlägerstr. 38, 64289 Darmstadt, Germany.
3. D. F. Alferov, Yu. A. Bashmakov, K. A. Belovintsev, E. G. Bessonov, and P. A. Cherenkov, *The Ondulator as a Source of Electromagnetic Radiation*, Particle Accelerators, vol. 9, pp 223-236, 1979.
4. J. E. Spencer and H. Winick, *Wiggler Systems as Sources of Electromagnetic Radiation*, in *Synchrotron Radiation Research*, edited by H. Winick and S. Doniach, Plenum Press, New York, 1980
5. L. A. Gevorgyan, N. A. Korkhmazyan, Sov. Phys. Tech. Phys., vol. 49, No. 11, p. 1400, 1979.
6. B. M. Kincaid, J. Opt. Soc. Am. B/Vol. 2, No. 8, August 1985.
7. R. M. Barnett *et al*, Phys. Rev. D54, No. 1, 1996.
8. R. Coisson, Phys. Rev. A, vol. 20 No. 2, p. 524, 1979.